Iterative precision measurement of branching ratios applied to 5P States in [superscript 88]Sr[superscript +]

Iterative precision measurement of branching ratios applied to 5*P* states in $^{88}Sr^{+}$

2016 New J. Phys. 18 123021

(http://iopscience.iop.org/1367-2630/18/12/123021)

New Journal of Physics
The open access journal at the forefront of physics

Deutsche Physikalische Gesellschaft DPG
IOP Institute of Physics

Published in partnership with: Deutsche Physikalische Gesellschaft and the Institute of Physics

PAPER

OPEN ACCESS

RECEIVED
27 October 2016

REVISED
28 November 2016

ACCEPTED FOR PUBLICATION
1 December 2016

PUBLISHED
15 December 2016

Iterative precision measurement of branching ratios applied to 5*P* states in $^{88}Sr^{+}$

Helena Zhang, Michael Gutierrez, Guang Hao Low, Richard Rines, Jules Stuart, Tailin Wu and Isaac Chuang[1]

MIT-Harvard Center for Ultracold Atoms, Department of Physics, Massachusetts Institute of Technology, Cambridge, MA 02139, USA
[1] Author to whom any correspondence should be adressed.

E-mail: ichuang@mit.edu

Keywords: properties of atoms, ion trapping, precision measurement, branching ratios and oscillator strengths

Abstract

We report and demonstrate a method for measuring the branching ratios of dipole transitions of trapped atomic ions by performing nested sequences of population inversions. This scheme is broadly applicable to species with metastable lambda systems and can be generalized to find the branching of any state to lowest states. It does not use ultrafast pulsed or narrow linewidth lasers and is insensitive to experimental variables such as laser and magnetic field noise as well as ion heating. To demonstrate its effectiveness, we make the most accurate measurements thus far of the branching ratios of both $5P_{1/2}$ and $5P_{3/2}$ states in $^{88}Sr^{+}$ with sub-1% uncertainties. We measure 17.175(27) for the $5P_{1/2}$–$5S_{1/2}$ branching ratio, 15.845(71) for $5P_{3/2}$–$5S_{1/2}$, and 0.056 09(21) for $5P_{3/2}$–$4D_{5/2}$. These values represent the first precision measurement for $5P_{3/2}$–$4D_{5/2}$, as well as ten- and thirty-fold improvements in precision respectively for $5P_{1/2}$–$5S_{1/2}$ and $5P_{3/2}$–$5S_{1/2}$ over the best previous experimental values.

1. Introduction

Empirical measurements of physical constants are fundamental to the verification and advancement of our knowledge of atoms. One important atomic property is the branching ratio of an electronic transition $E \rightarrow G$:

$$\mathrm{BR}(E \rightarrow G) = \frac{A_{E\rightarrow G}}{\sum_{S\in F} A_{E\rightarrow S} - A_{E\rightarrow G}}, \quad (1)$$

where A is the transition rate and F is the set of all states E directly decays to. Measuring these constants accurately is vital for the refinement of relativistic many-body theories and provides a crucial probe in the study of fundamental physics such as parity non-conservation [1–6].

Branching ratios for different atomic species are of great use in a wide range of fields including astrophysics, where analyzing the composition of stars contributes greatly to understanding stellar formation and evolution. Abundances of heavy elements such as strontium are essential for determining the efficiency of neutron capture processes in metal-poor stars, yet can be difficult to determine from emission spectra due to nearby transitions of other elements [7–13]. Branching ratios of these transitions are therefore vital for quantitative modeling of nucleosynthesis processes [11–13].

In addition, precise branching ratios enable the improvement of clock standards, paving the way for better global positioning systems and tests of the time-invariance of fundamental constants [14]. Atomic clocks using the optical quadrupole transition $5S_{1/2}$–$4D_{5/2}$ in $^{88}Sr^{+}$, one of the secondary clock standards recommended by the International Committee for Weights and Measures [14], have achieved uncertainties at the 10^{-17} level [15], more accurate than the current ^{133}Cs clock standard [16]. To further improve the precision of these systems, it is necessary to reduce uncertainty from the blackbody radiation Stark shift, a dominant source of error in many clock systems [2]. Branching ratios measured below the 1% level, combined with high-precision lifetime measurements, can improve the accuracy of static polarizabilities of clock states in $^{88}Sr^{+}$ and many systems and

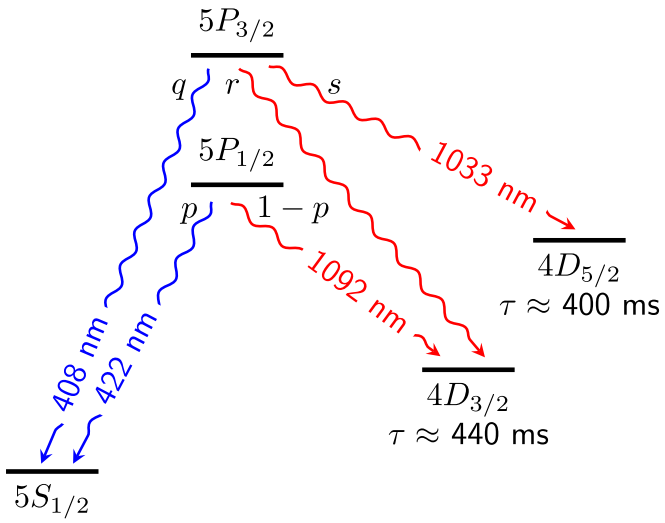

Figure 1. Energy levels of $^{88}Sr^{+}$, showing the $5P_{1/2}$ and $5P_{3/2}$ excited states and their decay channels. $4D_{3/2}$ and $4D_{5/2}$ are metastable states with lifetimes much greater than the timescale of the experiment [26]. To measure the $5P_{3/2}$ branching ratio, we need only lasers addressing the 408, 422, 1092, and 1033 nm transitions.

thereby reduce the uncertainty in blackbody radiation shift error, in addition to providing a verification against other methods for determining polarizability [2, 17].

Despite their relevance, branching ratios of heavy atoms have not been precisely measured for many decades due to the large uncertainties inherent in traditional discharge chamber methods using the Hanle effect [18]. Recent astrophysical studies still use these older experimental results for fitting emission spectra [12, 13]. Only in the last decade have there been measurements of branching ratios at the 1% level [19–22] using trapped ions, which are versatile toolkits for precision spectroscopy [4, 15, 23] as well as quantum computation [24]. In particular, Ramm *et al* [19] established a simple method for measuring branching ratios of $P_{1/2}$ states in trapped ions with metastable lambda systems.

Here, we present a novel scheme for measuring the branching ratios of the $P_{3/2}$ state of a trapped ion with an iterative population transfer sequence, significantly extending Ramm *et al*'s method. As with [19], we do not require ultrafast pulsed lasers or narrow linewidth lasers for addressing quadrupole transitions, which were used by previous precision measurements of $P_{3/2}$ branching ratios [21, 25]. Our method uses only two lasers that pump the ion from the ground state to the $P_{1/2}$ and $P_{3/2}$ excited states and two lasers to unshelve the ion from the metastable states below $P_{3/2}$. For $^{88}Sr^{+}$ and analogous species, these dipole-addressing lasers are already used for Doppler cooling, making this scheme broadly applicable for many trapped ion systems without the need for additional equipment. Like [19], our method is insensitive to experimental variables such as magnetic field and laser fluctuations. Furthermore, we show that the method can be extended to measure the branching ratios of an arbitrary excited state to the ground and metastable states through all intermediate states. We demonstrate the effectiveness of this method by making the first precision measurement of the $5P_{3/2}$–$4D_{5/2}$ and $5P_{3/2}$–$4D_{3/2}$ branching ratios in $^{88}Sr^{+}$ in addition to the most accurate measurement of the $5P_{1/2}$ branching ratios to date.

2. Iterative branching ratio measurement

We begin by briefly describing the procedure for measuring branching ratios of $P_{1/2}$ states in metastable lambda systems using the method by Ramm *et al*, which will be a building block for the $P_{3/2}$ system. We use the $5P_{1/2}$ excited state in $^{88}Sr^{+}$ as the model system (figure 1), and denote the probability of decaying to the ground $5S_{1/2}$ state as p and the long-lived $4D_{3/2}$ state as $1 - p$.

At the start of the experiment, the ion is initialized to the ground $5S_{1/2}$ state. In the first step, the 422 nm laser is turned on to optically pump the ion to the excited $5P_{1/2}$ state while we record ion fluorescence at 422 nm. In the process of the ion fully shelving to the metastable $4D_{3/2}$ state, we detect a mean number of photons $\langle n \rangle = \epsilon_{422} \cdot p/(1 - p)$, where ϵ_{422} is the detection efficiency of our system at 422 nm [19]. In the second step, the 1092 nm laser is turned on to repump the ion to the excited state, during which we detect ϵ_{422} photon as it decays to the $5S_{1/2}$ state. The branching ratio $p/(1 - p)$ is therefore equal to the ratio of the number of photons observed during the two time intervals, independent of the collection efficiency.

For the more complex $5P_{3/2}$ state, which decays to three instead of two states, we denote the probability of decaying to the $5S_{1/2}$, $4D_{3/2}$, and $4D_{5/2}$ states as q, r, and $s = 1 - q - r$ respectively (figure 1). To measure the

$5P_{3/2}$ branching ratios $q/(1-q)$, $r/(1-r)$, and $s/(1-s)$, we begin with a sequence analogous to the $5P_{1/2}$ sequence, this time detecting photons at both 408 and 422 nm. Starting again with the ion in the $5S_{1/2}$ ground state, we first pump the ion into the excited $5P_{3/2}$ state with the 408 nm laser (Step A). We detect a mean number of photons from the ion

$$\langle N_{\mathrm{A}}\rangle = \epsilon_{408}\frac{q}{1-q}, \tag{2}$$

where ϵ_{408} is the detection efficiency at 408 nm. We now turn on the 1033 nm laser, which drives the ion to the $5P_{3/2}$ state if it was in the $4D_{5/2}$ state and does nothing otherwise (Step B). We detect a mean number of 408 nm photons

$$\langle N_{\mathrm{B}}\rangle = \epsilon_{408}\frac{qs}{(1-q)(1-s)} \tag{3}$$

in this step. We can obtain the $5P_{3/2}$–$4D_{5/2}$ branching ratio $s/(1-s)$ from the photon count ratio of the previous two steps.

To measure the other two branching ratios, we note that their values are contained in the state of the ion after Step B—the population split between the $5S_{1/2}$ and $4D_{3/2}$ states. To obtain this information, we now turn on the 422 nm laser to pump all $5S_{1/2}$ population into the $4D_{3/2}$ state (Step C). We detect

$$\langle N_{\mathrm{C}}\rangle = \epsilon_{422}\frac{qs}{(1-q)(1-s)}\frac{p}{1-p} \tag{4}$$

photons at 422 nm. Finally, turning on the 1092 nm laser repumps all of the population to the $5S_{1/2}$ state and we detect $\langle N_{\mathrm{D}}\rangle = \epsilon_{422}$ photon (Step D), which is necessary for canceling the detection efficiency ϵ_{422}.

Since we can determine p experimentally with the $5P_{1/2}$ branching ratio sequence, we can solve for the $5P_{3/2}$ branching ratios without knowing ϵ_{422} or ϵ_{408}:

$$\frac{s}{1-s} = \frac{\langle N_{\mathrm{B}}\rangle}{\langle N_{\mathrm{A}}\rangle}, \tag{5}$$

$$\frac{q}{1-q} = \frac{\langle N_{\mathrm{A}}\rangle\langle N_{\mathrm{C}}\rangle}{\langle N_{\mathrm{B}}\rangle\langle N_{\mathrm{D}}\rangle}\frac{1-p}{p}. \tag{6}$$

As with the $P_{1/2}$ measurement scheme by Ramm *et al*, our sequence of population transfers is insensitive to detection efficiencies and most experimental variables. The long-lived shelving states $4D_{3/2}$ and $4D_{5/2}$ allow for the length of the measurement to far exceed the timescale needed for population transfer, rendering the measurement independent of laser power and frequency fluctuations as well as ion heating. There are no coherence effects or dark resonances since only one laser is on at a time, so our method is also insensitive to micromotion and magnetic field fluctuations. This distinguishes our method from a proposed $P_{3/2}$ branching ratio measurement scheme [27], which not only requires an extra laser for the $5P_{3/2}$–$4D_{3/2}$ transition but also that two lasers be alternately pulsed for each step to avoid dark resonances, making the measurement sequence significantly longer.

The branching ratios of states higher than $5P_{3/2}$ to the ground state and metastable D states are also of practical importance for calculating the scalar polarizability [2] as well as improving elemental abundance models of stars [13]. Our iterative method can be generalized to find the branching of any excited state to the lowest five states in $^{88}Sr^{+}$ through any number of intermediate states (see appendix). This also enables the full branching ratios of many higher states to be determined in $^{88}Sr^{+}$ and analogous species.

3. Experimental measurement in $^{88}Sr^{+}$

To demonstrate our iterative method, we experimentally measure the $5P_{1/2}$ and $5P_{3/2}$ branching ratios in $^{88}Sr^{+}$ using a trapped ion system to levels of precision over an order of magnitude over previous best values.

3.1. Experimental procedure

We trap single $^{88}Sr^{+}$ ions using a surface electrode Paul trap fabricated by Sandia National Laboratories [28]. RF and DC confining fields are set such that the axial secular frequency of the ion is 600 kHz, with radial frequencies in the 3–4 MHz range and a 15° tilt in the radial plane. A magnetic field of 5.4 G is applied normal to the trap to lift the degeneracy of the Zeeman states [29]. Fluorescence from the ion is collected along the same axis by an in-vacuum 0.42 NA aspheric lens (Edmunds 49-696) into a single photon resolution photomultiplier tube (PMT, Hamamatsu H10682-210) with a filter that only passes light between 408 and 422 nm (Semrock FF01-415/10-25). The PMT signal is counted by an FPGA with arrival time binned into 2 ns intervals. The overall detection efficiency of the setup is approximately 4×10^{-3} at both 422 and 408 nm. Dipole transitions of the ion are

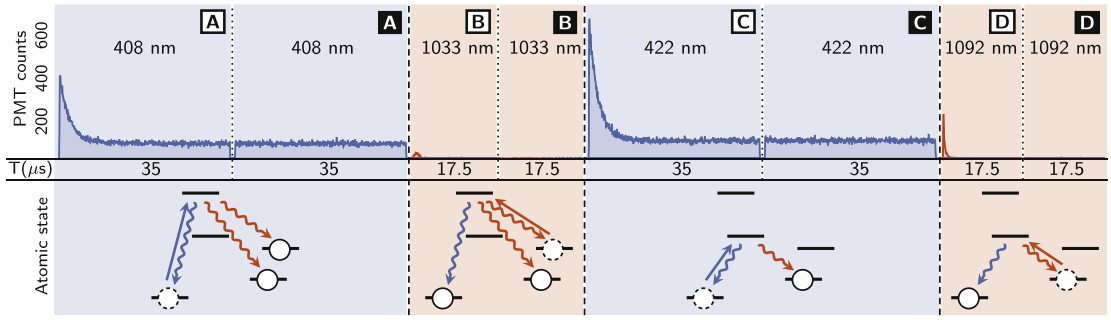

Figure 2. Real time-resolved fluorescence collected from the ion at 422 and 408 nm after 8×10^6 cycles of the $5P_{3/2}$ branching ratio data sequence. Counts in the background intervals (black ABCD squares) are subtracted from the data intervals (white ABCD squares) to obtain only fluorescence from the ion for each step. The length T of each interval is indicated, and the laser turn-off time is 1 μs between each interval. Atomic states losing population (dashed circle) and gaining population (solid circle) during each step are depicted.

addressed using frequency-stabilized diode lasers. To execute the experimental sequence, we switch laser beams on and off using acousto-optic modulators (AOMs) driven by FPGA-controlled direct digital synthesizers.

Each branching ratio measurement cycle begins with 100 μs of Doppler cooling using 422 and 1092 nm lasers. Subsequently, we turn on only the 1092 nm laser for 20 μs to ensure the ion is in the $5S_{1/2}$ state, then perform the experimental sequence. We ran the $5P_{1/2}$ and $5P_{3/2}$ branching ratio measurement sequences for 1.9×10^8 and 6.4×10^7 cycles respectively for a run time of 13 and 6 h each. For each step within the experimental sequence, the laser is turned on twice: first the data interval where population transfer occurs, then the background interval that is subtracted from the data interval to obtain only fluorescence from the ion. For the $5P_{1/2}$ experiment, the 422 nm and 1092 nm intervals are 35 μs and 25 μs in length respectively for both data and background, with 1 μs between each interval, and the $5P_{3/2}$ experimental sequence is depicted in figure 2.

3.2. Error analysis

To correct for systematic effects on branching ratios, we carefully calibrated the sources of error in our experiment, which are summarized in table 1.

The polarization alignment error arises from the Hanle effect and is a function of the magnetic field, detector position, and incident laser direction and polarization. In the $5P_{1/2}$ system, the $m = \pm 1/2$ sublevels both emit radiation isotropically with 1:2 ratios of π- to σ-polarized light regardless of magnetic and electric fields, so this does not affect the measurement [30]. However, the Hanle effect is a major source of error for the $5P_{3/2}$ system as the ratio of emitted π- to σ-polarized photons is 0:1 for $m = \pm 3/2$ sublevels and 2:1 for $m = \pm 1/2$ sublevels. The ratio of π to σ light emitted from Step A and Step B will therefore not be equal in general, biasing the fluorescence ratio.

To resolve this problem, we linearly polarize 408 and 1033 nm light to an axis set at $\arctan(\sqrt{2}) \approx 54.7°$ (the magic angle [31]) with respect to the magnetic field, which is set orthogonally to the laser beam. At the magic angle, the ratio of π- to σ- polarized light emitted during Steps A and B are both equal to 1:2. The difference between radiation patterns of π and σ photons and any birefringence effects in the detection system cancel out. We use a Glan-Taylor polarizer (Thorlabs GT10) with >50 dB attenuation of the orthogonal polarization to align the 408 and 1033 nm laser polarizations to within 0.2° of the magic angle. We measured the effective phase retardance $\Delta\phi$ due to possible birefringence of optics and vacuum window after the polarizer to be <0.02 radians at both blue and infrared wavelengths, which does not contribute significantly to the uncertainties. The error in aligning the laser polarization with respect to the magnetic field and setting the magnetic field to be orthogonal to the laser beam accounts for the polarization alignment error in table 1.

The effects of the other sources of systematics are accounted for by modeling the time-resolved fluorescence curves using optical Bloch equations to determine the shift and uncertainty contributed by each error source. PMT dead time, calibrated to be 20 ± 1 ns for our system using the method by Meeks and Siegel [32], leads to more undercounting in steps with higher count rates. Finite laser durations reduce the fluorescence from the ion in each step in addition to preparing states imperfectly. The small amount of laser light still present when the AOMs are switched off (extinction ratios >60 dB) leads to slight coupling between undesirable states. The finite lifetimes of the $4D_{3/2}$ and $4D_{5/2}$ states lead to extra counts in the blue intervals and reduced counts in the IR intervals. Off-resonant excitations, where the ion is excited to the wrong state by a collision or far-detuned laser, are found to contribute negligible errors to our system based on measuring the frequency of dark events while Doppler cooling the ion. We find that these sources of systematics do not limit our current level of precision. We

Table 1. List of systematic sources of error for branching ratios of $5P_{1/2}$–$5S_{1/2}$, $5P_{3/2}$–$5S_{1/2}$, and $5P_{3/2}$–$4D_{5/2}$ and their fractional contributions to the overall shift and uncertainty. Powers of 10 are in brackets.

	Fractional shift and uncertainty		
Error source	$p/(1-p)$	$q/(1-q)$	$s/(1-s)$
Counting statistics	$\pm 16[-4]$	$\pm 38[-4]$	$\pm 33[-4]$
Polarization alignment	—	$\pm 19[-4]$	$\pm 19[-4]$
PMT dead time	$46 \pm 2[-5]$	$76 \pm 5[-5]$	$-45 \pm 1[-5]$
Finite laser durations	$13 \pm 9[-8]$	$\pm 3[-6]$	$-6 \pm 2[-6]$
AOM extinction ratio	$\pm 7[-7]$	$\pm 3[-6]$	$\pm 1[-6]$
Finite D state lifetime	$354 \pm 4[-8]$	$-40 \pm 2[-7]$	$-124 \pm 2[-7]$
$5P_{1/2}$ branching ratio	—	$\pm 16[-4]$	—
Total	$5 \pm 16[-4]$	$8 \pm 45[-4]$	$5 \pm 38[-4]$

also verify that the fluorescence from the ion is normally distributed when binned into successive 500 000 measurement cycles.

The largest source of error for both $5P_{1/2}$ and $5P_{3/2}$ branching ratios is from counting statistics. This can be improved via either more measurement cycles, more ions, or greater collection efficiency, though for the latter two methods it is important to take into account the increased error from PMT dead time. Other errors can also be reduced via improvement of the experimental apparatus, such as more accurate alignment of the laser polarization and using a PMT with less dead time. The only fundamental limitation to the accuracy of the technique is the uncertainty on the finite lifetimes of the $4D_{3/2}$ and $4D_{5/2}$ states, which restricts the length of the population inversion sequence, but the limit is many orders of magnitude below the current level of accuracy.

After correcting for systematic shifts and propagating uncertainties, we obtain for the $5P_{1/2}$ branching ratio $p/(1-p) = 17.175(27)$ and for the $5P_{3/2}$ branching ratios $q/(1-q) = 15.845(71)$, $r/(1-r) = 0.0063(4)$, and $s/(1-s) = 0.056\,09(21)$, with errors representing 1σ bounds. The corresponding branching fractions are $p = 0.944\,98(8), 1-p = 0.055\,02(8)$, $q = 0.9406(2)$, $r = 0.0063(3)$, and $s = 0.0531(2)$.

3.3. Comparison with previous works

The uncertainty of our results is at a level smaller than the discrepancy between previous experimental and theoretical results, as shown in figure 3. Our value for the $5P_{1/2}$–$5S_{1/2}$ branching ratio is in agreement with the recent measurement done by Likforman *et al* [20] with trapped ions, as well as theoretical values of Safronova [1] and Jiang *et al* [2], while it is 1.9 σ away from the gas discharge chamber experiment by Gallagher [18]. For $5P_{3/2}$, only the $5P_{3/2}$–$5S_{1/2}$ branching ratio has been previously reported, also by Gallagher, which our value is in agreement with. We are also in agreement with theory values of Safronova and Jiang *et al* for all $5P_{3/2}$ branching ratios. We note that Safronova's theoretical values have been found to be in good agreement with precision measurements of branching ratios and dipole matrix elements in other elements [19, 23, 33–35]. We obtain a ten-fold improvement in precision for the $5P_{1/2}$ branching ratios over Likforman *et al* and a thirty-fold improvement for the $5P_{3/2}$–$5S_{1/2}$ branching ratio over the early results of Gallagher.

For improving the precision of $^{88}Sr^{+}$ atomic clocks, it is important to have accurate rates for transitions to the $4D_{5/2}$ and $5S_{1/2}$ levels. Using the 6.63(7) ns $5P_{3/2}$ lifetime value measured by Pinnington *et al* [36], we obtain transition rates $A_{P_{3/2}-S_{1/2}} = 1.425(15) \times 10^{8}\ s^{-1}$ and $A_{P_{3/2}-D_{5/2}} = 8.010(89) \times 10^{6}\ s^{-1}$ using our measured branching ratios. These are significantly more accurate compared to previous best-known transition rates of $A_{P_{3/2}-S_{1/2}} = 1.43(6) \times 10^{8}\ s^{-1}$ and $A_{P_{3/2}-D_{5/2}} = 8.7(1.5) \times 10^{6}\ s^{-1}$ from Gallagher [18]. The uncertainty in transition rates is now dominated by the uncertainty in the $5P_{3/2}$ lifetime.

4. Conclusion and outlook

In summary, we have introduced a novel method for measuring the branching ratio of the $P_{3/2}$ state in ions with metastable lambda systems and demonstrated its effectiveness with measurements in $^{88}Sr^{+}$ at the sub-1% level. Our scheme, as with the Ramm *et al* method for $P_{1/2}$ states, uses only dipole transition addressing lasers and is insensitive to detector efficiencies, laser and magnetic field fluctuations, as well as ion heating and micromotion. We further describe how to extend this population transfer sequence to measure the branching of any excited state to the $P_{1/2}$, $P_{3/2}$, and ground and metastable states through all intermediate states with the addition of a few more lasers. This scheme is also broadly applicable to excited states in other elements with a similar lambda

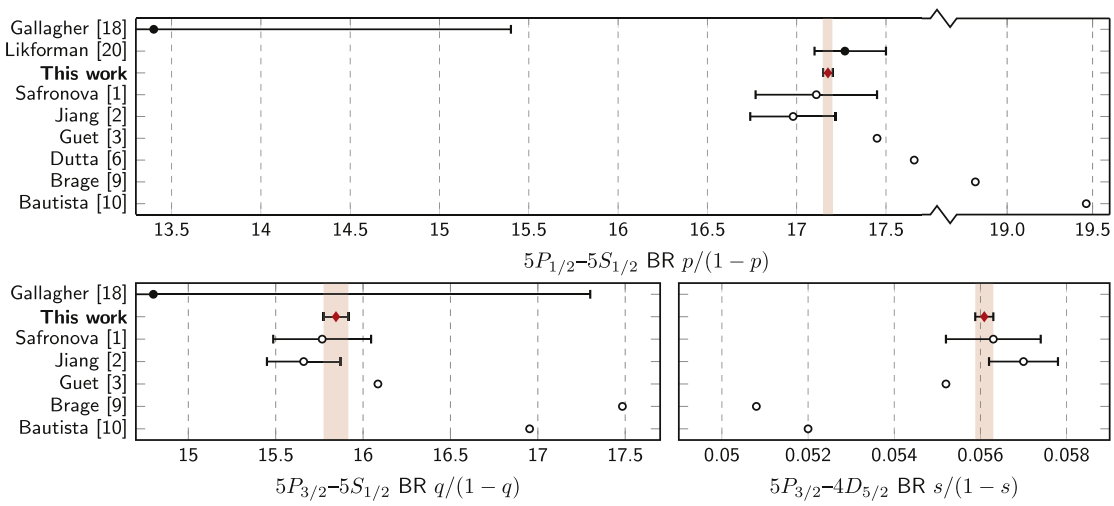

Figure 3. Branching ratios (BR) for the $5P_{1/2}$ and $5P_{3/2}$ excited states in Sr^+ obtained by this work (red diamond) and previous experimental (filled circle) and theoretical (empty circle) works. Error bars are included whenever uncertainties are provided by the source.

structure of decaying into a ground state and long-lived states, such as secondary clock standards $^{199}Hg^+$ and $^{171}Yb^+$, for which greater branching ratio and lifetime precision can reduce uncertainty from blackbody radiation as well [37, 38].

Acknowledgments

The authors acknowledge helpful discussions with Hartmut Häffner, Christian Roos, and Luca Guidoni. This work was supported in part by the IARPA MQCO program and by the NSF Center for Ultracold Atoms.

Appendix. Generalization of branching ratio measurement to arbitrary excited states

Denote the set of the five lowermost states in $^{88}Sr^+$, $5S_{1/2}$, $5P_{3/2}$, $5P_{1/2}$, $4D_{3/2}$, and $4D_{5/2}$, as S. Define the set of all states that state E decays to through any number of intermediate states to be $T(E)$. We define the *base branching fraction* $\mathrm{BBF}(E, A)$ of $E \to A$ for $A \in S$ to be the probability of state E decaying to A while only ever occupying intermediate states from the set $T(E) - S$. We label the base branching fractions of E to $5S_{1/2}$, $5P_{3/2}$, $5P_{1/2}$, $4D_{3/2}$, and $4D_{5/2}$ to be a, b, c, d, and $e = 1 - a - b - c - d$ respectively, as shown in figure A1 .

It follows that $\sum_{A\in S} \mathrm{BBF}(E, A) = 1$, as all end states (ground and metastable) of $^{88}Sr^+$ are in S. We define *base branching ratios* to be $\mathrm{BBR}(E, A) = \mathrm{BBF}(E, A)/(1 - \mathrm{BBF}(E, A))$. Under the assumption that E and all states in $T(E) - S$ decay much faster than the lifetime of $4D_{3/2}$ and $4D_{5/2}$, it is possible to measure base branching ratios of any E.

As all higher states of $^{88}Sr^+$ have nonzero probability of eventually decay to $5P_{1/2}$ or $5P_{3/2}$, there will always be 422 or 408 nm photons emitted after the ion is excited to E. In fact, base branching ratios can be measured by the same experimental setup for measuring $P_{3/2}$ branching ratios, with the addition of appropriate dipole-addressing lasers as well as the minor modification of detecting 422 and 408 nm photons separately. A scheme which solves for the base branching ratios of any state $E \notin S$ is as follows:

(i) Pump the ion from $5S_{1/2}$ to E, collect $\langle N_1 \rangle$ photons total, $\langle N_1^{408} \rangle$ at 408 nm and $\langle N_1^{422} \rangle$ at 422 nm.

(ii) Pump from $4D_{5/2}$ to E, collect $\langle N_2 \rangle$ photons total, $\langle N_2^{408} \rangle$ at 408 nm and $\langle N_2^{422} \rangle$ photons at 422 nm.

(iii) Pump from $4D_{3/2}$ to $5P_{1/2}$, collect $\langle N_3^{422} \rangle$ photons.

(iv) Pump the ion from $5S_{1/2}$ to E.

(v) Pump from $4D_{5/2}$ to $5P_{3/2}$, collect $\langle N_4^{408} \rangle$ photons.

(vi) Pump from $4D_{3/2}$ to $5P_{1/2}$, collect $\langle N_5^{422} \rangle$ photons.

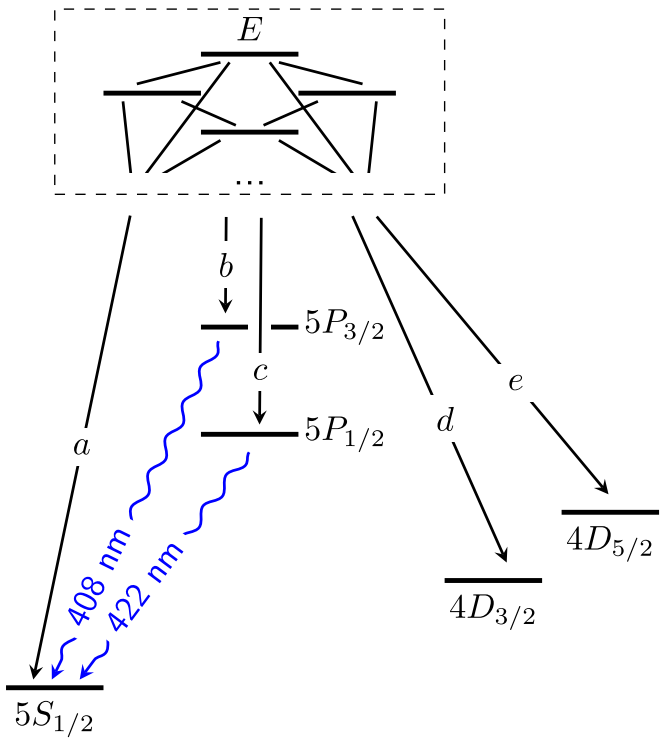

Figure A1. The base branching ratios of an arbitrary state E in $^{88}Sr^{+}$, effectively the branching ratios of the set of states consisting of E and all states higher than the five lowermost states that E decays to. Only detecting 422 and 408 nm photons from various population transfers is sufficient for measuring base branching ratios.

The base branching ratios can be calculated from the experimental results as follows:

$$\begin{aligned}\frac{a}{1-a} = \{&q(\langle N_1^{408}\rangle\langle N_2\rangle - \langle N_1\rangle\langle N_4^{408}\rangle)(\langle N_1\rangle\langle N_3^{422}\rangle - (\langle N_1\rangle + \langle N_2\rangle)\langle N_5^{422}\rangle)\\ &- r(\langle N_1\rangle + \langle N_2\rangle)\langle N_4^{408}\rangle[\langle N_2\rangle\langle N_1^{422}\rangle + \langle N_1\rangle(\langle N_3^{422}\rangle - \langle N_5^{422}\rangle)]\}/\\ &\{q\langle N_2\rangle(\langle N_1^{408}\rangle + \langle N_4^{408}\rangle)[(\langle N_1\rangle + \langle N_2\rangle)\langle N_5^{422}\rangle - \langle N_1\rangle\langle N_3^{422}\rangle]\\ &+ r\langle N_2\rangle(\langle N_1\rangle + \langle N_2\rangle)\langle N_4^{408}\rangle(\langle N_1^{422}\rangle + \langle N_5^{422}\rangle)\},\end{aligned} \tag{A.1}$$

$$\frac{b}{1-b} = \frac{\langle N_1^{408}\rangle\langle N_2\rangle}{(q+r)\langle N_4^{408}\rangle(\langle N_1\rangle + \langle N_2\rangle) - \langle N_1^{408}\rangle\langle N_2\rangle}, \tag{A.2}$$

$$\frac{c}{1-c} = \frac{r\langle N_1^{422}\rangle\langle N_2\rangle}{p(q+r)\langle N_1\rangle(\langle N_5^{422}\rangle - \langle N_3^{422}\rangle) - \langle N_2\rangle(r\langle N_1^{422}\rangle - p(q+r)\langle N_5^{422}\rangle)}, \tag{A.3}$$

$$\frac{e}{1-e} = \frac{\langle N_2\rangle[(q+r)\langle N_4^{408}\rangle - s\langle N_1^{408}\rangle]}{(q+r)\langle N_1\rangle\langle N_4^{408}\rangle + s\langle N_1^{408}\rangle\langle N_2\rangle}. \tag{A.4}$$

This scheme is insensitive to the same experimental variables as the $5P_{3/2}$ measurement scheme. Aside from the lasers needed for transferring the ion population from $5S_{1/2}$ and $4D_{5/2}$ to E, no other additional equipment is necessary. With some adjustments, it can be used to solve for base branching ratios of other analogous species with long-lived metastable states.

References

[1] Safronova U 2010 *Phys. Rev.* A **82** 022504
[2] Jiang D, Arora B, Safronova M and Clark C W 2009 *J. Phys.* B **42** 154020
[3] Guet C and Johnson W 1991 *Phys. Rev.* A **44** 1531
[4] Fortson N 1993 *Phys. Rev. Lett.* **70** 2383
[5] Dzuba V and Flambaum V 2011 *Phys. Rev.* A **83** 052513
[6] Dutta N N and Majumder S 2014 *Phys. Rev.* A **90** 012522
[7] Caffau E, Andrievsky S, Korotin S, Origlia L, Oliva E, Sanna N, Ludwig H G and Bonifacio P 2016 *Astron. Astrophys.* **585** A16
[8] Hansen T *et al* 2014 *Astrophys. J.* **787** 162
[9] Brage T, Wahlgren G M, Johansson S G, Leckrone D S and Proffitt C R 1998 *Astrophys. J.* **496** 1051
[10] Bautista M, Gull T, Ishibashi K, Hartman H and Davidson K 2002 *Mon. Not. R. Astron. Soc.* **331** 875–9
[11] Gratton R and Sneden C 1994 *Astron. Astrophys.* **287** 927–46

[12] Siqueira-Mello C, Andrievsky S, Barbuy B, Spite M, Spite F and Korotin S 2015 *Astron. Astrophys.* **584** A86
[13] Bergemann M, Hansen C, Bautista M and Ruchti G 2012 *Astron. Astrophys.* **546** A90
[14] Ludlow A D, Boyd M M, Ye J, Peik E and Schmidt P O 2015 *Rev. Mod. Phys.* **87** 637
[15] Madej A A, Dubé P, Zhou Z, Bernard J E and Gertsvolf M 2012 *Phys. Rev. Lett.* **109** 203002
[16] Weyers S, Gerginov V, Nemitz N, Li R and Gibble K 2011 *Metrologia* **49** 82
[17] Dubé P, Madej A A, Tibbo M and Bernard J E 2014 *Phys. Rev. Lett.* **112** 173002
[18] Gallagher A 1967 *Phys. Rev.* **157** 24
[19] Ramm M, Pruttivarasin T, Kokish M, Talukdar I and Häffner H 2013 *Phys. Rev. Lett.* **111** 023004
[20] Likforman J P, Tugayé V, Guibal S and Guidoni L 2016 *Phys. Rev.* A **93** 052507
[21] Gerritsma R, Kirchmair G, Zähringer F, Benhelm J, Blatt R and Roos C 2008 *Eur. Phys. J. D* **50** 13–9
[22] De Munshi D, Dutta T, Rebhi R and Mukherjee M 2015 *Phys. Rev.* A **91** 040501
[23] Hettrich M, Ruster T, Kaufmann H, Roos C, Schmiegelow C, Schmidt-Kaler F and Poschinger U 2015 *Phys. Rev. Lett.* **115** 143003
[24] Monz T, Nigg D, Martinez E A, Brandl M F, Schindler P, Rines R, Wang S X, Chuang I L and Blatt R 2016 *Science* **351** 1068–70
[25] Kurz N, Dietrich M, Shu G, Bowler R, Salacka J, Mirgon V and Blinov B 2008 *Phys. Rev.* A **77** 060501
[26] Sahoo B, Islam M R, Das B, Chaudhuri R and Mukherjee D 2006 *Phys. Rev.* A **74** 062504
[27] Pruttivarasin T 2014 *PhD Thesis* University of California, Berkeley
[28] Clark C *et al* 2013 *Bull. Am. Phys. Soc.* **58** 6
[29] Berkeland D and Boshier M 2002 *Phys. Rev.* A **65** 033413
[30] Gallagher A and Lurio A 1963 *Phys. Rev. Lett.* **10** 25
[31] Fano U and Macek J H 1973 *Rev. Mod. Phys.* **45** 553
[32] Meeks C and Siegel P 2008 *Am. J. Phys.* **76** 589–90
[33] Auchter C, Noel T W, Hoffman M R, Williams S R and Blinov B B 2014 *Phys. Rev.* A **90** 060501
[34] Safronova M and Safronova U 2011 *Phys. Rev.* A **83** 012503
[35] Safronova U and Safronova M 2011 *Can. J. Phys.* **89** 465–72
[36] Pinnington E, Berends R and Lumsden M 1995 *J. Phys.* B **28** 2095
[37] Oskay W *et al* 2006 *Phys. Rev. Lett.* **97** 020801
[38] Huntemann N, Sanner C, Lipphardt B, Tamm C and Peik E 2016 *Phys. Rev. Lett.* **116** 063001